Geomechanics and Engineering, *Vol. 36, No. 5 (2024) 489-509*
https://doi.org/10.12989/gae.2024.36.5.489

Prediction of rock slope failure using multiple ML algorithms

Bowen Liu*[1], Zhenwei Wang[1], Sabih Hashim Muhodir[2], Abed Alanazi[3], Shtwai Alsubai[3] and Abdullah Alqahtani[4]

[1]*School of Civil Engineering, North China University of Technology, Beijing 100144, China*
[2]*Department of Architectural Engineering, Cihan University-Erbil, Kurdistan Region, Iraq*
[3]*Department of Computer Science, College of Computer Engineering and Sciences in Al-Kharj, Prince Sattam bin Abdulaziz University, P.O. Box 151, Al-Kharj 11942, Saudi Arabia*
[4]*Software Engineering Department, College of Computer Engineering and Sciences, Prince Sattam bin Abdulaziz University, P.O. Box 151, Al-Kharj 11942, Saudi Arabia*

(*Received November 19, 2023, Revised February 19, 2024, Accepted February 20, 2024*)

Abstract. Slope stability analysis and prediction are of critical importance to geotechnical engineers, given the severe consequences associated with slope failure. This research endeavors to forecast the factor of safety (FOS) for slopes through the implementation of six distinct ML techniques, including back propagation neural networks (BPNN), feed-forward neural networks (FFNN), Takagi-Sugeno fuzzy system (TSF), gene expression programming (GEP), and least-square support vector machine (Ls-SVM). 344 slope cases were analyzed, incorporating a variety of geometric and shear strength parameters measured through the PLAXIS software alongside several loss functions to assess the models' performance. The findings demonstrated that all models produced satisfactory results, with BPNN and GEP models proving to be the most precise, achieving an R^2 of 0.86 each and MAE and MAPE rates of 0.00012 and 0.00002 and 0.005 and 0.004, respectively. A Pearson correlation and residuals statistical analysis were carried out to examine the importance of each factor in the prediction, revealing that all considered geomechanical features are significantly relevant to slope stability. However, the parameters of friction angle and slope height were found to be the most and least significant, respectively. In addition, to aid in the FOS computation for engineering challenges, a graphical user interface (GUI) for the ML-based techniques was created .

Keywords: factor of safety; graphical user interface; ML; PLAXIS; slope stability

1. Introduction

Geotechnical engineering strives for a comprehensive understanding of slope stability analysis in light of growing economic transformations in landscapes. Landslide events resulting from slope instability rank as some of the most devastating natural disasters globally, following only behind earthquakes and volcanoes. Preventing or mitigating such occurrences necessitates a profound appreciation for the significance of slope stability analysis that considers multiple variables, including, but not limited to, slope angle, height, soil properties, and fluctuating soil water content (Pantelidis 2009, Suman *et al.* 2016).

However, while such variables may contribute to slope instability in distinct ways, their significance depends on a combination of factors such as soil type, vegetation, and climate change among others. Furthermore, not all factors carry an equal weight in contributing to slope stability, with diverse factors impacting the stability of slopes to varying degrees depending on soil composition and the surrounding environment. Therefore, there is a crucial need for geotechnical engineers to consider the complexity of slope stability analysis to mitigate the devastating consequences of slope instability (Eberhardt 2003).

Significant global research efforts have been devoted to predicting and assessing slope stability, with various empirical, numerical, mathematical, and experimental approaches to analyze and anticipate slope failures. However, despite noteworthy progress, these approaches are not entirely free of limitations and are only suitable for specific slope stability problems. Hence, further approaches may still be required to fully address the issue of slope stability.

The current methods employed for slope stability analysis have limitations such as the inability of the limit equilibrium method to consider the soil constitutive relationships and the arduous nature of analyzing multi-layer soils. This approach is inadequate for precisely predicting safety and reliability during slope stability analysis. Moreover, the inconsistency in defining the safety factor means that slopes possessing a factor of safety (FOS) greater than 1.20 can still fail in practical scenarios. In addition, human subjectivity can also impact the accuracy of slope stability analysis methods, especially those that entail expert judgments.

Therefore, a more comprehensive, accurate, and reliable approach is necessary to overcome the limitations of existing methods and accurately predict potential slope failures. A multitude of supervised learning approaches are accessible for slope stability computation, with several studies demonstrating remarkable results (Liu and Chen 2007). Thus, the assessment uncertainties in FOS values

*Corresponding author, Ph.D.
E-mail: lang860930@126.com

ISSN: 2005-307X (Print), 2092-6219 (Online)

Table 1 Studies on the slope stability predictions using ML and deep learning neural networks

References	Input(s)	Output	Computing machinery methods	Dataset no
Lu and Rosenbaum (2003)	ϒ, H, φ, C, α, ru		ANN	32
Wang *et al.* (2005)	ϒ, H, φ, C, α, C		ANN	27
Samui (2008)	ϒ, H, φ, C, α, ru		SVM	46
Das *et al*. (2011)	ϒ, H, φ, C, α, ru		ANN	46
Liu *et al*. (2014)	ϒ, H, φ, C, α, ru	FOS	ELM	97
Hoang and Pham (2016)	ϒ, H, φ, C, α, ru		Ls-SVR	168
Mahmoodzadeh *et al*. (2021)	ϒ, H, φ, C, α, ru		KNN, SVR, GPR, DT, LSTM, DNN	327
Ahangari et al. (2022)	ϒ, H, φ, C, α,		MLP, SVM, KNN, DT, RF	70
Present study	ϒ, H, φ, C, α, ru		TSF, FFNN, BPNN, GEP, MVR, Ls-SVM	344

represent a significant challenge for conventional stability analysis methods. This problem has been addressed by researchers who have turned to computational intelligence approaches. In recent years, machine learning (ML) techniques have gained increasing attention due to their ability to reduce uncertainties.

Lu and Rosenbaum (2003) developed a method that combined artificial neural networks (ANN) and the gray system technique to analyze slope stability based on geotechnical features and historical behavior. Zhao *et al.* (2012) used the relevance vector machine (RVM) to explore the correlation between slope stability and relevant factors, while Liu *et al*. (2014) assessed 97 cases using the extreme learning machine (ELM) method. Moreover, Samui (2008) and Li *et al.* (2013) used support vector machine (SVM) to evaluate slope stability with promising results and also projected slope stability using SVM with favorable outcomes. Hoang and Pham (2016) implemented the metaheuristic optimization of least squares support vector regression (Ls-SVR) for slope analysis utilizing 168 data points. Jagan *et al.* (2016) employed several learning classifiers, such as adaptive neuro fuzzy inference system (ANFIS), GPR, RVM, and ELM, to assess layered slope stability. Chakraborty and Goswami (2017) employed the MLP model to estimate the factor of safety and cross-validated their results using numerical finite element codes. Omar *et al*. (2021) leveraged MLP- and ANFIS-based predictive models, along with LEMs, to scrutinize the stability of a layered slope, yielding dependable FOS evaluations. Mahmoodzadeh *et al*. (2021) applied six ML techniques to predict FOS based on 327 data points.

Bai *et al*. (2022) developed and compared ML-based predictive models for FOS forecasting for slopes, demonstrating their successful application for stability analysis. Karir *et al*. (2022) employed a variety of ML models to forecast and obtain FOS values for both natural and man-made slopes.

As a summarize, Table 1 shows several studies that leverage the power of soft computational methods to forecast slope stability through the circular failure mode. As can be seen in this table and literature review, there are some limitations which are modified in this paper.

One of them is related to the application of methods. Several researches were just considered simple neural networks, whereas, vast methods based on artificial intelligence (AI) were developed to predict the output factors such as genetic algorithms, fuzzy-based systems, and neural network with advanced features. To overcome this limitation, in this paper six supervised and unsupervised methods are used for prediction of FOS, which are covered all types of computing machinery techniques.

The second one is about the number of data. As can be seen, some of works were just considered a small number of data. However, this work utilizes 344 slope cases from Iran, which is more than the most of previous studies.

The third aspect pertains to the utilization of statistical methods. It is important to note that while intelligent models have been employed in explaining slope failures, they may not always offer complete solutions as a specific approach may only be suitable for certain circumstances. Moreover, validating the accuracy and reliability of these models necessitates further investigation. A clear distinction between different intelligent modeling techniques used to forecast slope stability is yet to be established, which negatively affects their credibility and precision. To enhance model performance, it is advised to incorporate various statistical methods such as probability-probability (P-P) and quantile-quantile (Q-Q) plots, analysis of variance (ANOVA), Durbin-Watson analysis, Pearson correlation, collinearity checks, Casewise diagnostics, and loss functions. These techniques, which were not considered in previous research, are all implemented in the current study.

Overall, to forecast FOS, six unsupervised and supervised ML methods were utilized in this study, specifically multi-variable regression (MVR), back propagation neural network (BPNN), feed-forward neural network (FFNN), Takagi-Sugeno fuzzy system (TSF), gene expression programming (GEP), and least-square support vector machine (Ls-SVM). Input parameters, including cohesion (c), slope angle (α), unit weight (ϒ), slope height (h), friction angle (φ), and pore pressure ratio (r_u), were measured from 344 slope cases in Iran using PLAXIS software. Pearson correlation of unsupervised regression and other statistical methods were used to identify the most critical factors influencing slope stability. Fig. 1 depicts the flowchart of this work.

2. Database development

Fig. 2 illustrates a slope's geometry and important parameters that affect its stability. It is important to note that

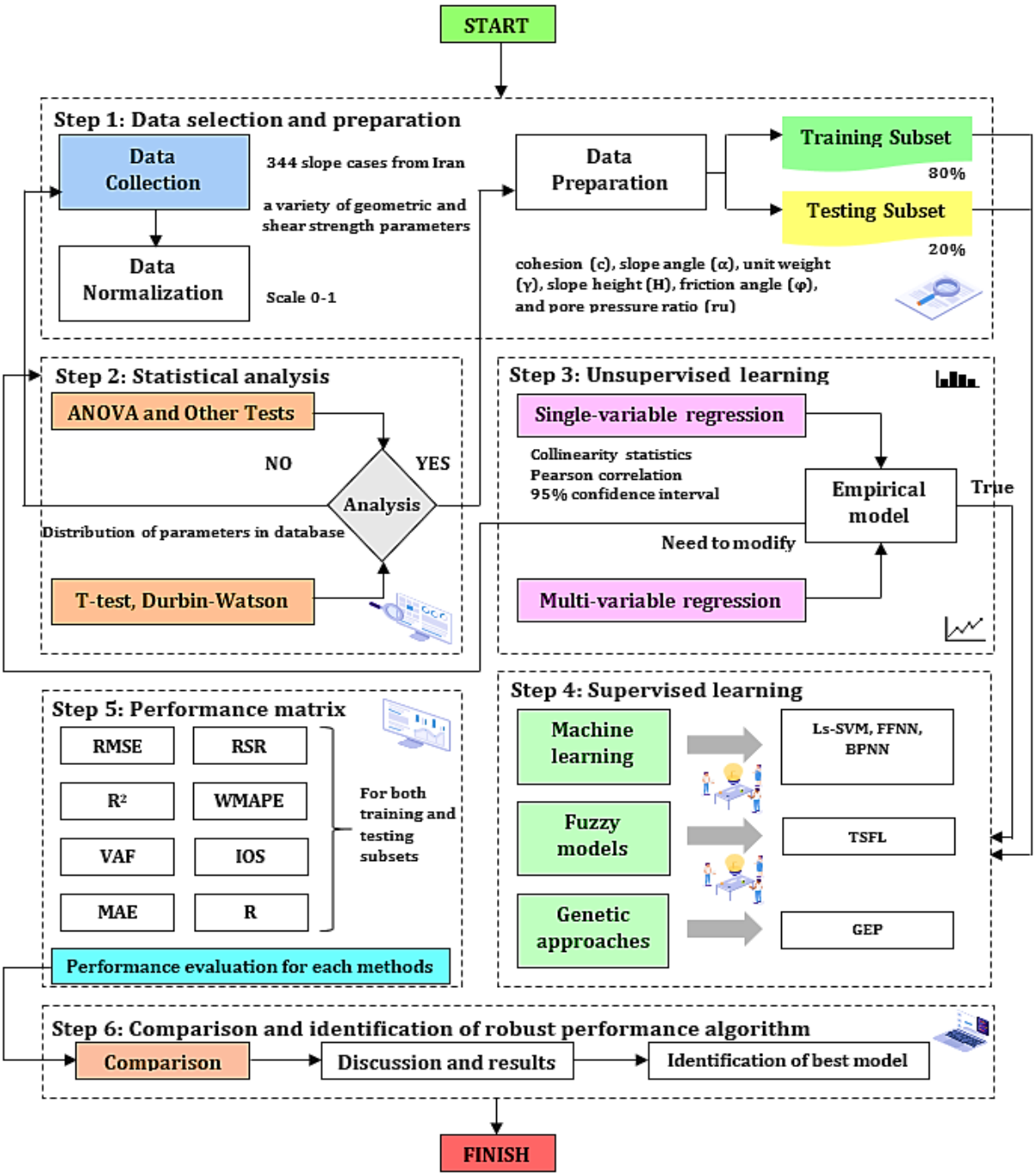

Fig. 1 Flowchart of slope stability prediction using unsupervised and supervised techniques

this study only considers internal factors that contribute to slope failure, disregarding external factors such as human-made factors and the effects of earthquakes. This figure vividly elucidates the complex relationship between a slope's geometric characteristics and the critical parameters that significantly impact its stability with regard to sliding surfaces.

In the majority of previous studies, six factors, namely c, α, ϒ, H, φ, and r_u, were identified as significant factors affecting slope stability.

The researchers in this study utilized a comprehensive database encompassing slope heights ranging from 3 to 565 meters, which allows for a thorough exploration of the various factors affecting slope stability. This wide range of values for slope heights provides a robust foundation for drawing meaningful conclusions and insights.

This study examines the geotechnical strength parameters for evaluation, specifically focusing on two geological strength factors: cohesion and internal friction angle of materials. The study identifies the range of cohesion as 0-200 kPa, and the internal friction angle as 0-45 degrees. These parameters and their respective range of values are deemed reliable and acceptable factors for determining the geotechnical strength parameters of rock slopes.

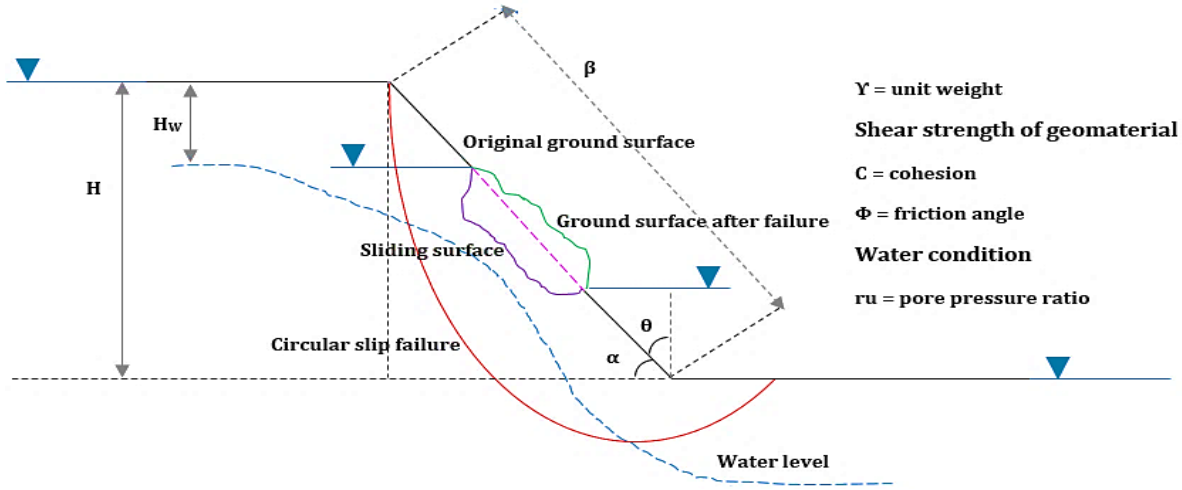

Fig. 2 Slope configuration and factors influencing slope stability

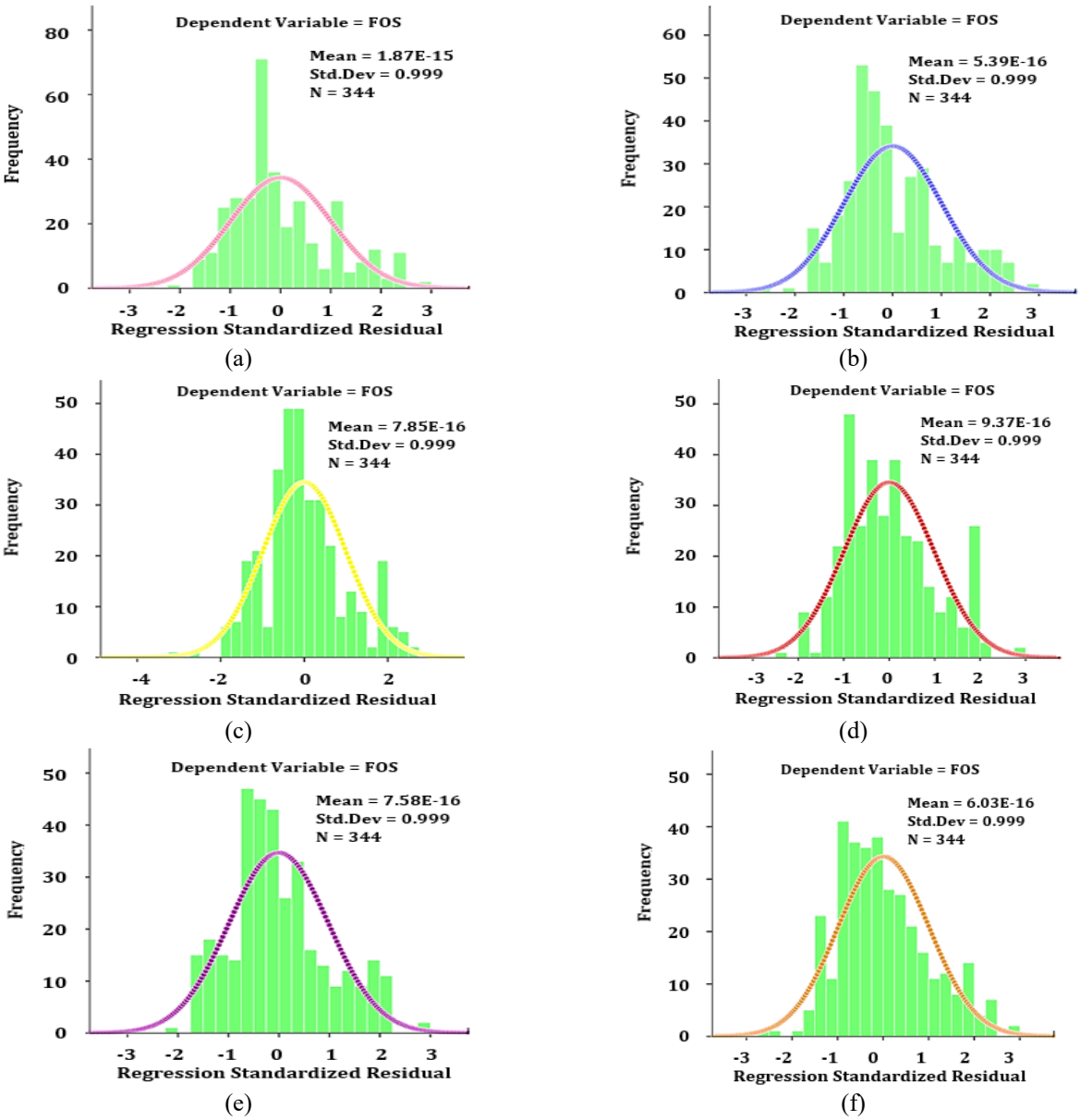

Fig. 3 Distribution histograms of parameters in the database (a) ϒ, (b) c, (c) φ, (d) α, (e) H and (f) r_u.

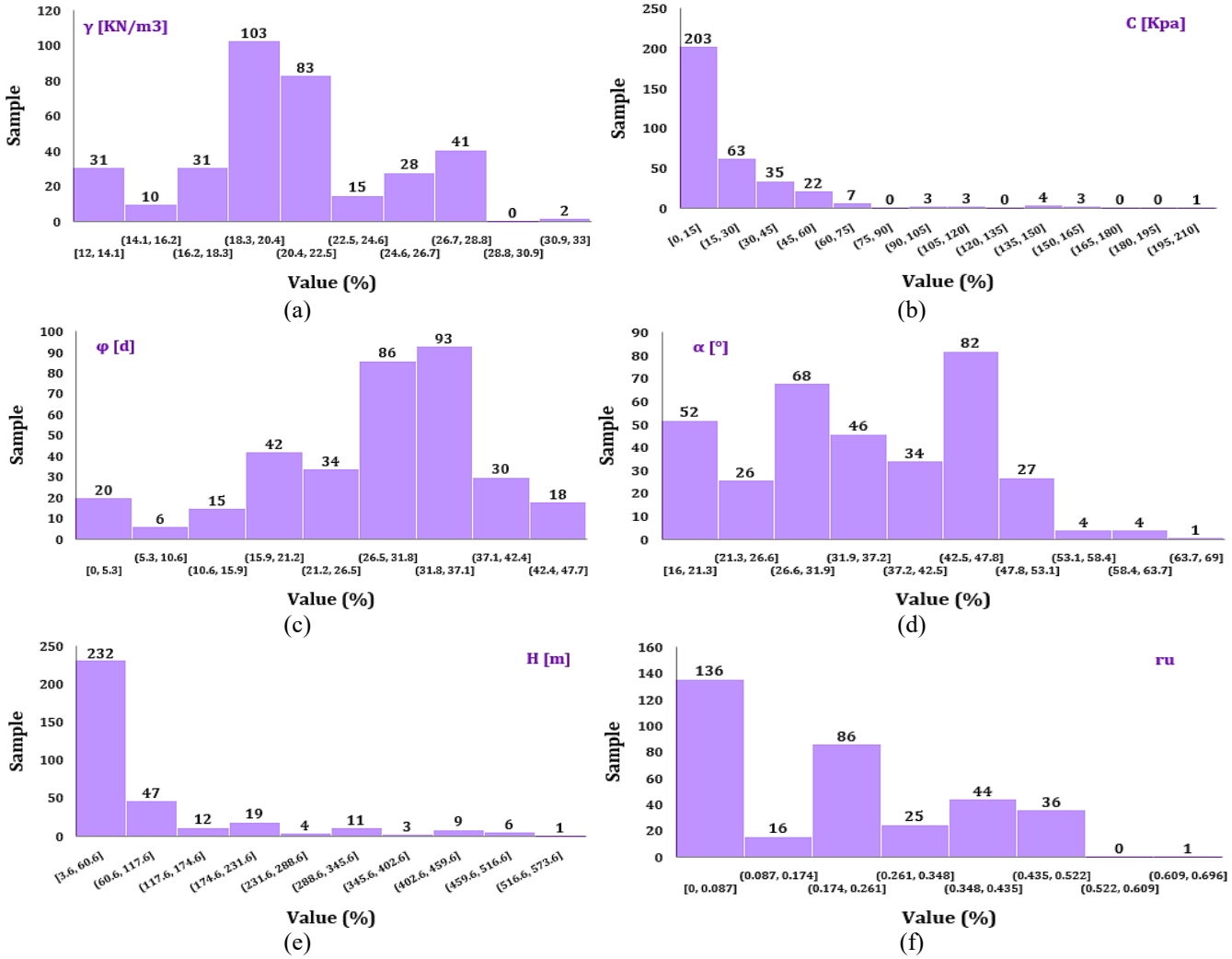

Fig. 4 Distribution and frequency histograms of input parameters (a) ϒ, (b) c, (c) φ, (d) α, (e) H and (f) r_u.

Table 2 Overview of statistical findings for recorded database parameters

Par	Unit weight	Cohesion	Friction angle	Slope angle	Slope height	Pore pressure ratio	FOS
Sym	ϒ	c	φ	α	H	r_u	FOS
Unit	KN/m^3	KPa	d	°	m	-	-
Count	344.00	344.00	344.00	344.00	344.00	344.00	344
Min	13.5	0.00	0.00	17.00	3.60	0.00	0.24
Max	27.94	55.95	45.00	66.00	565.00	0.45	2.31
Var	17.08	851.27	111.63	112.21	12779.56	0.03	0.14
Std. V	4.13	29.18	10.57	10.59	113.05	0.17	0.37
Sqrt	4.54	4.03	5.15	5.48	6.32	0.00	1.12
Kurt	-0.12	10.79	0.92	-0.86	4.39	-1.24	-0.07

Therefore, following the existing literature and the availability of data, these six factors were taken into account in this study. To evaluate the reliability of the prediction models applied to assess slope stability, a comprehensive database consisting of 344 slope cases analyzed for circular failure mechanisms was utilized.

The dataset consists of 344 observations of rock slope stability gathered from various open-pit mines in Iran. In this context, cohesion and internal friction angle of rock materials along the slopes are utilized as strengths for geotechnical parameters, while unit weight serves as a physical parameter for properties of rock materials. The aforementioned parameters are crucial for understanding the behavior and stability of rock slopes, particularly in the context of potential failure criteria. Despite the absence of explicit utilization of rock failure criteria in the study, the

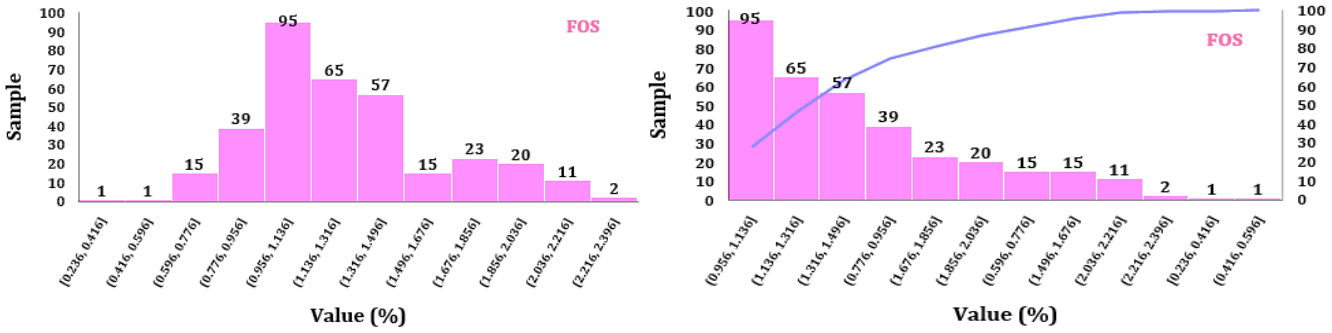

Fig. 5 Frequency and Pareto histograms of output parameter (FOS)

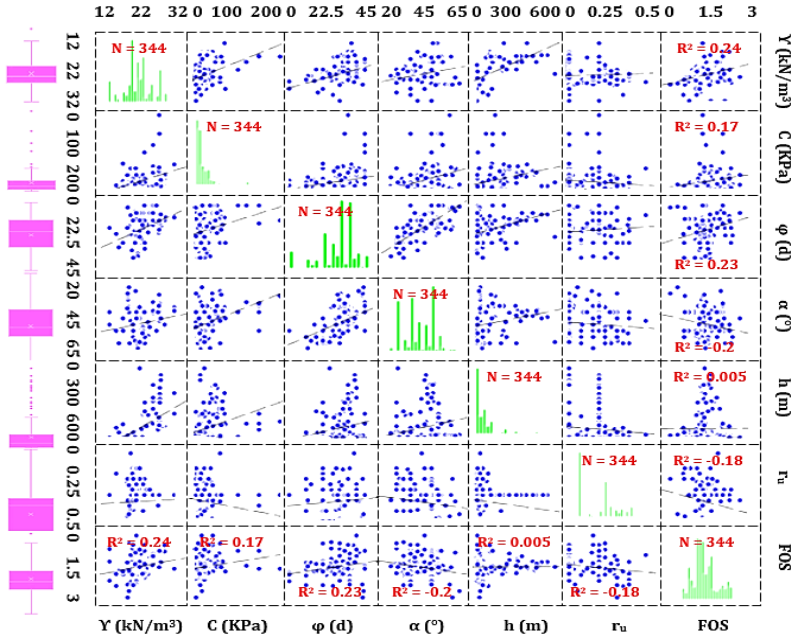

Fig. 6 The scatterplot matrix of parameters

analysis of geotechnical and physical parameters provides valuable insights into the characteristics of rock slopes and their potential for stability or failure.

Circular failure is a commonly occurring type of slope failure in soil and more fractured rock areas. FOS values were obtained by analyzing all slopes using the finite element software PLAXIS, and the outcomes were compared with the predictions made by the soft computing models.

The threshold is FOS = 1.37. All the 344 slope cases are from real slopes in Iran. For the facilitation of researcher access to our database, a hyperlink is furnished within the Data Availability section, enabling the retrieval of the requisite data.

The present study utilizes correlation and basic descriptive statistics to attain a more profound comprehension of the used database. Figs. 3 and 4 shows the histograms and distribution of the monitored geotechnical and physical properties of materials as input variables and also FOS as output variable. Also, the Pareto and normal histogram of FOS are indicated in Fig. 5. In addition, Table 2 presents the statistical indices of the comprehensive dataset. To illustrate the linear relationships between the dependent variable (FOS) and the independent variables, which consist of geometric and shear strength parameters of soil materials, a scatterplot matrix and Box graph are displayed in Fig. 6.

3. Results and analysis

3.1 Statistical analysis

In this study, both individual correlation and multiple-variable regression analyses were conducted to explore the connections and associations among soil strength parameters, physical properties, and FOS in order to formulate novel empirical equations in the concluding phase. The FOS exhibits a notable correlation with Υ, φ, α, while displaying a weaker correlation with H and c. Fig. 7 illustrates the normal probability-probability (P-P) plot of standardized residuals from the regression analysis for each input parameter. Fig. 8 displays the standardized residuals from the regression analysis aligned with the standardized

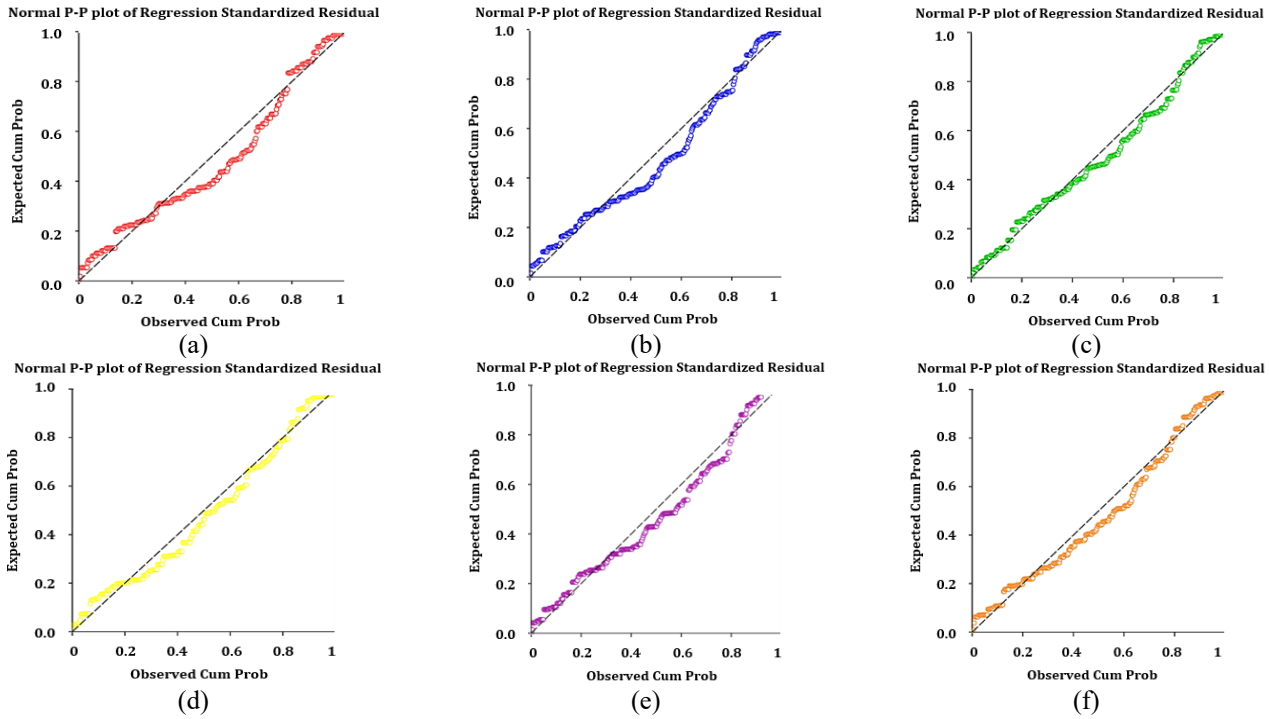

Fig. 7 Standardized residuals P-P plot for regression analysis (a) ϒ, (b) c, (c) φ, (d) α, (e) H and (f) r_u.

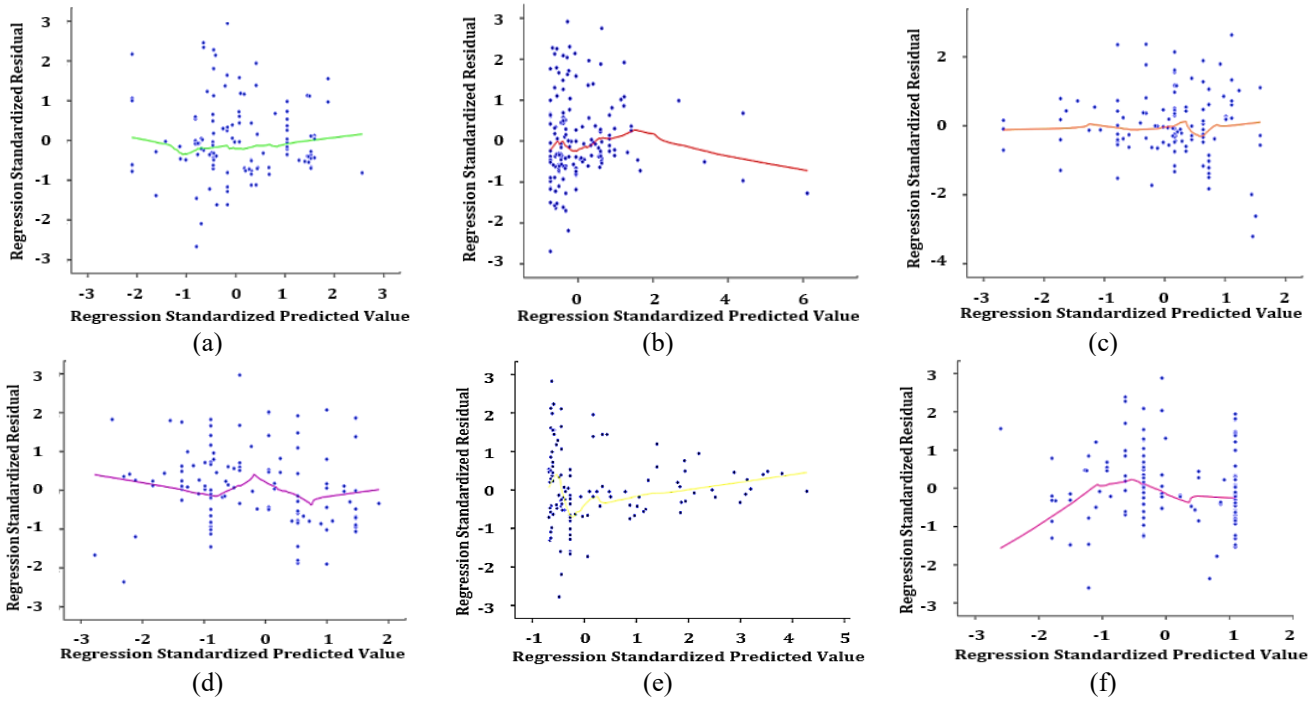

Fig. 8 Relationship between Standardized Residuals and Standardized Predicted Values in Regression (a) ϒ, (b) c, (c) φ, (d) α, (e) H and (f) r_u

predicted values for each specified independent variable. Also, Fig. 9 shows a normal quantile-quantile (Q-Q) plot of each input variables. All of these statistical diagrams indicate reliable results to predict FOS. As can be seen, the results of inputs are close and fit to x=y line, which presents results with high accuracy in terms of statistics.

For more clarification and showing the results of Q-Q plot and P-P plot as numerical data, Tables 3-8 presents the results of residuals statistical including predicted values, residuals, distances, statistical influences, prediction intervals, and some others for each input parameters (cohesion, slope angle, unit weight, slope height, friction angle, and pore pressure ratio) based on some statistical indices (minimum, maximum, mean, standard deviation).

Table 3 The results of residuals statistical for unit weight (ϒ)

	Minimum	Maximum	Mean	Std. Deviation	N
Forecasted value	1.079	1.492	1.265	0.088	344
Std. forecasted value	-2.100	2.563	0.000	1.000	344
Standard error of forecasted value	0.019	0.053	0.026	0.008	344
Adjusted forecasted value	1.066	1.498	1.265	0.088	344
Residual	-0.958	1.060	0.000	0.358	344
Std. residual	-2.668	2.951	0.000	0.999	344
Stud. residual	-2.674	2.955	0.000	1.001	344
Deleted residual	-0.963	1.063	0.000	0.360	344
Stud. deleted residual	-2.699	2.989	0.001	1.004	344
Mahal. distance	0.000	6.570	0.997	1.363	344
Cook's distance	0.000	0.038	0.003	0.004	344
Centered leverage value	0.000	0.019	0.003	0.004	344

Table 4 The results of residuals statistical for cohesion (c)

	Minimum	Maximum	Mean	Std. Deviation	N
Forecasted value	1.217	1.663	1.265	0.065	344
Std. forecasted value	-0.735	6.109	0.000	1.000	344
Standard error of forecasted value	0.020	0.122	0.025	0.012	344
Adjusted forecasted value	1.214	1.722	1.265	0.067	344
Residual	-0.981	1.063	0.000	0.363	344
Std. residual	-2.693	2.918	0.000	0.999	344
Stud. residual	-2.699	2.923	0.000	1.001	344
Deleted residual	-0.985	1.066	-0.000	0.365	344
Stud. deleted residual	-2.724	2.956	0.000	1.004	344
Mahal. distance	0.003	37.32	0.997	3.547	344
Cook's distance	0.000	0.115	0.003	0.008	344
Centered leverage value	0.000	0.109	0.003	0.010	344

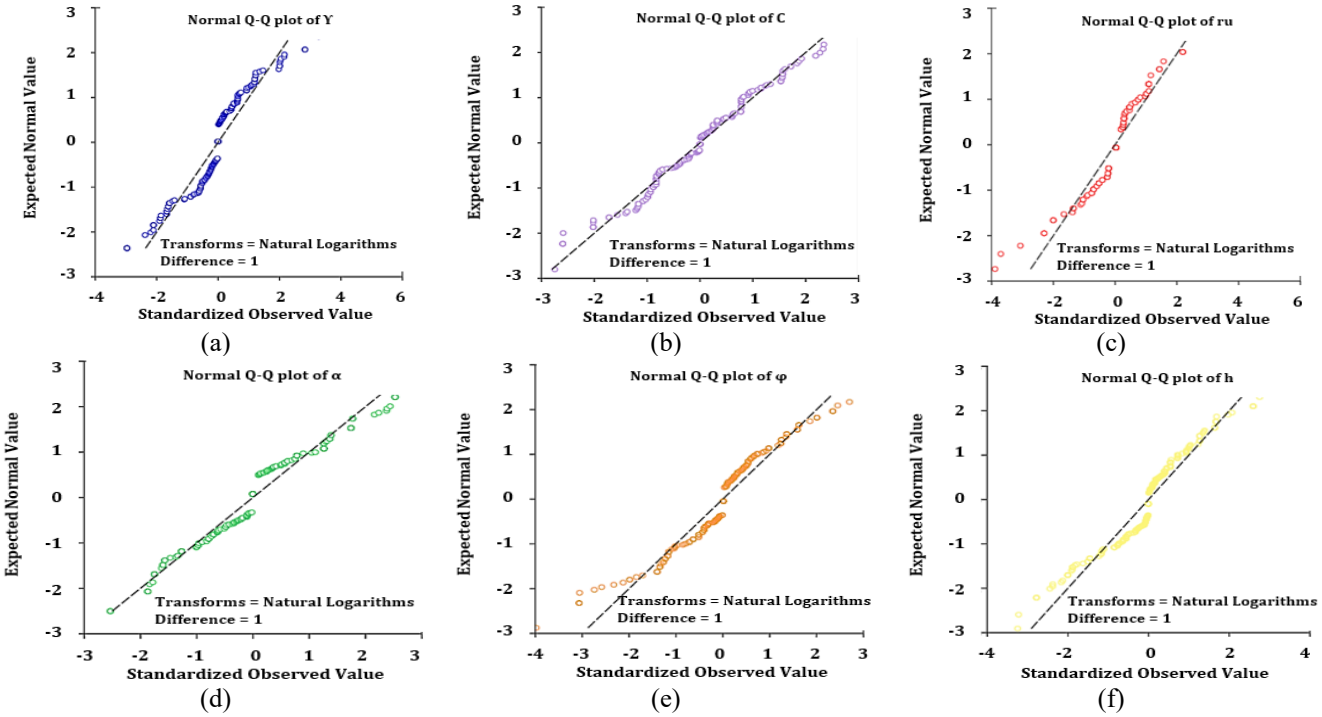

Fig. 9 Normal Q-Q plot of each input variables in the dataset. (a) ϒ, (b) c, (c) φ, (d) α, (e) H and (f) r_u

Table 5 The results of residuals statistical for friction angle (φ)

	Minimum	Maximum	Mean	Std. Deviation	N
Forecasted value	1.0338	1.401	1.265	0.086	344
Std. forecasted value	-2.672	1.580	0.000	1.000	344
Standard error of forecasted value	0.019	0.055	0.026	0.009	344
Adjusted forecasted value	1.032	1.404	1.265	0.086	344
Residual	-1.155	0.949	0.000	0.359	344
Std. residual	-3.211	2.638	0.000	0.999	344
Stud. residual	-3.225	2.646	0.000	1.001	344
Deleted residual	-1.165	0.955	-0.000	0.361	344
Stud. deleted residual	-3.271	2.670	0.000	1.004	344
Mahal. distance	0.001	7.142	0.997	1.696	344
Cook's distance	0.000	0.048	0.002	0.004	344
Centered leverage value	0.000	0.021	0.003	0.005	344

Table 6 The results of residuals statistical for slope angle (α)

	Minimum	Maximum	Mean	Std. Deviation	N
Forecasted value	1.056	1.403	1.265	0.075	344
Std. forecasted value	-2.776	1.843	0.000	1.000	344
Standard error of forecasted value	0.020	0.058	0.027	0.007	344
Adjusted forecasted value	1.063	1.404	1.265	0.074	344
Residual	-0.856	1.076	0.000	0.361	344
Std. residual	-2.363	2.970	0.000	0.999	344
Stud. residual	-2.385	2.975	0.000	1.001	344
Deleted residual	-0.872	1.080	-0.000	0.364	344
Stud. deleted residual	-2.401	3.010	0.001	1.004	344
Mahal. distance	0.003	7.706	0.997	1.066	344
Cook's distance	0.000	0.053	0.003	0.005	344
Centered leverage value	0.000	0.022	0.003	0.003	344

Table 7 The results of residuals statistical for slope height (H)

	Minimum	Maximum	Mean	Std. Deviation	N
Forecasted value	1.263	1.273	1.265	0.001	344
Std. forecasted value	-0.682	4.277	0.000	1.000	344
Standard error of forecasted value	0.020	0.088	0.026	0.011	344
Adjusted forecasted value	1.259	1.274	1.264	0.002	344
Residual	-1.028	1.046	0.000	0.369	344
Std. residual	-2.778	2.826	0.000	0.999	344
Stud. residual	-2.783	2.832	0.000	1.001	344
Deleted residual	-1.031	1.050	0.000	0.371	344
Stud. deleted residual	-2.811	2.862	0.001	1.003	344
Mahal. distance	0.001	18.29	0.997	2.509	344
Cook's distance	0.000	0.016	0.002	0.003	344
Centered leverage value	0.000	0.053	0.003	0.007	344

The values of these tables are achieved by linear regression analysis in IBM SPSS Statistics Data Editor.

Furthermore, three diagrams including histogram of regression standardized residual, Normal P-P plot of regression standardized residual, and regression standardized residual corresponded to regression standardized predicted values are presented in Fig. 10 for dependent parameter (FOS) as output factor based on six input parameters (independent variables). As shown in these diagrams, the results indicate the reliable outcomes with high accuracy in terms of statistics. Also, Table 9 presents the results of residuals statistical including predicted values, residuals, distances, statistical influences, prediction intervals, and some others for FOS considering six input factors.

Table 8 The results of residuals statistical for pore pressure ratio (r_u)

	Minimum	Maximum	Mean	Std. Deviation	N
Forecasted value	1.089	1.338	1.265	0.067	344
Std. forecasted value	-2.600	1.089	0.000	1.000	344
Standard error of forecasted value	0.020	0.055	0.027	0.006	344
Adjusted forecasted value	1.076	1.342	1.265	0.067	344
Residual	-0.947	1.049	0.000	0.363	344
Std. residual	-2.602	2.883	0.000	0.999	344
Stud. residual	-2.612	2.888	0.000	1.001	344
Deleted residual	-0.953	1.052	-0.000	0.365	344
Stud. deleted residual	-2.634	2.919	0.001	1.004	344
Mahal. distance	0.000	6.762	0.997	0.869	344
Cook's distance	0.000	0.029	0.003	0.004	344
Centered leverage value	0.000	0.020	0.003	0.003	344

Table 9 The results of residuals statistical for FOS

	Minimum	Maximum	Mean	Std. Deviation	N
Forecasted value	0.786	2.048	1.265	0.235	344
Std. forecasted value	-2.034	3.326	0.000	1.000	344
Standard error of forecasted value	0.020	0.101	0.039	0.011	344
Adjusted forecasted value	0.786	2.134	1.265	0.237	344
Residual	-0.848	0.906	0.000	0.284	344
Std. residual	-2.951	3.156	0.000	0.991	344
Stud. residual	-3.098	3.171	0.000	1.003	344
Deleted residual	-0.934	0.915	-0.000	0.291	344
Stud. deleted residual	-3.139	3.215	0.000	1.006	344
Mahal. distance	0.670	41.36	5.983	4.597	344
Cook's distance	0.000	0.140	0.003	0.009	344
Centered leverage value	0.002	0.121	0.017	0.013	344

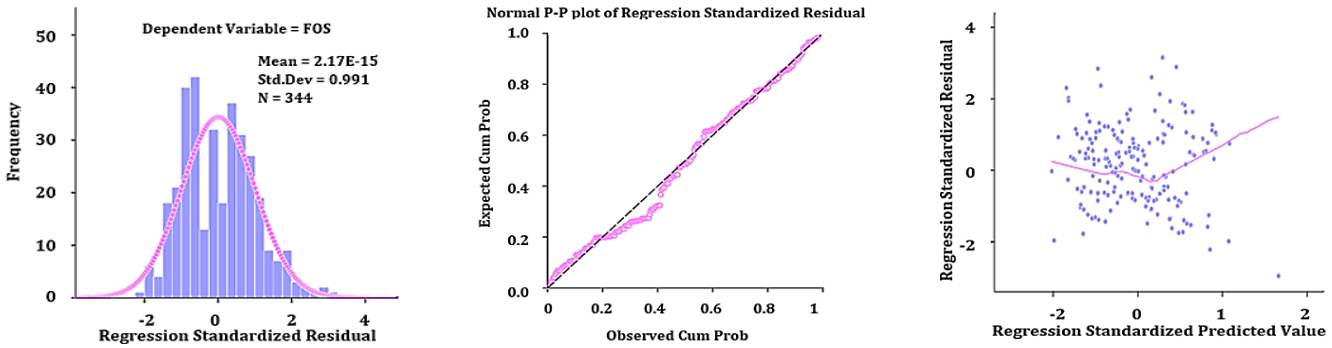

(a) (b) (c)

Fig. 10 Statistical diagrams for dependent parameter (FOS) as output factor

The development of a new empirical equation (Eq. (1)) that incorporates physical and geotechnical parameters of slopes is a significant advancement in slope stability analysis. Traditionally, stability analysis tools have relied on simplistic equations or simplified assumptions that may not accurately capture the complex interplay of geological, physical, and environmental factors that contribute to slope stability. By integrating a wide range of parameters into a single empirical equation, the new approach in this study provides a more comprehensive and accurate analysis of slope stability.

In the context of multi-variable regression analysis, six geotechnical and geometric parameters are utilized as independent variables, while the FOS serves as the dependent variable to evaluate the impact of each parameter on the FOS through forward stepwise regression (FSR) analysis. Table 10 presents the results of the ANOVA, Casewise diagnostics, and relevant statistical metrics associated with the derived formula for assessing FOS. The ANOVA outcomes and regression coefficients displayed in

Table 10 Analysis of variance results and model variables for predicting FOS

Model summary					
R	R Square	Adjusted R Square	Std. Error of the Estimate		Durbin-Watson
0.63	0.40	0.39	0.28		1.40
ANOVA analysis					
	Sum of Squares	df	Mean Square	F	Sig.
Regression	19.01	6	3.16	38.37	.000
Residual	27.83	337	0.08		
Total	46.84	343			

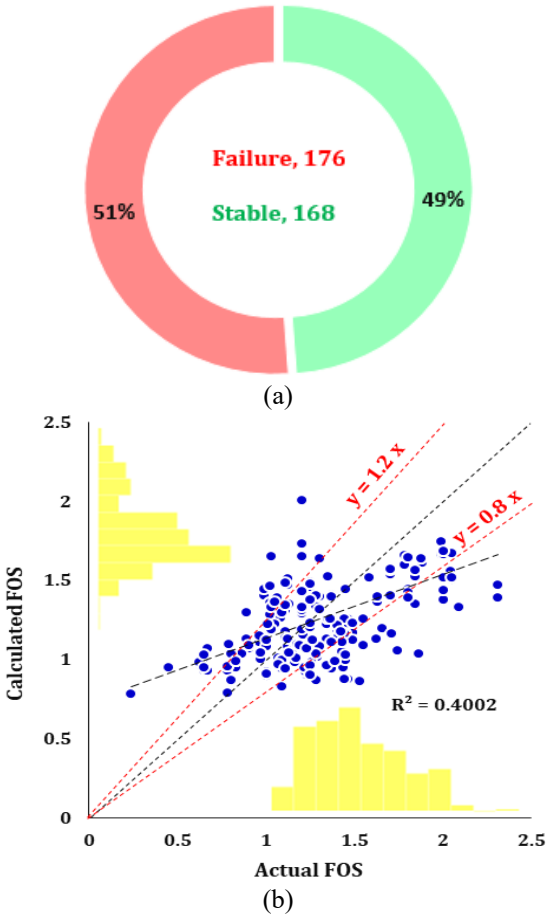

Fig. 11 (a) Doughnut chart of all slope cases and (b) correlation between calculated and measured FOS

Table 10 are deemed valid and satisfactory for the development of new models aimed at predicting FOS. Upon evaluation of collinearity statistics and covariance analysis, it is confirmed that the correlations and coefficients considered are accurate. Eq. (1) outlines the proposed empirical formula for calculating FOS.

$$FOS = \zeta + A + B + C$$
$$A = 0.003\,C + 0.019\,\varphi$$
$$B = 0.019\,\Upsilon - 0.665\,r_u \quad (1)$$
$$C = -0.022\,\alpha - 0.001\,H$$
$$\zeta = 1.237$$

Table 11 Evaluation of loss functions in establishing an empirical model for FOS

Loss functions	Value
RMSE	0.0004
MAE	0.0002
R^2	0.4000
R	0.6300
MAPE	0.0194
WMAPE	0.1221
VAF	11.7046
PI	0.5166
RSR	0.1390
NS	-94.2711
BF	0.0035
IOS	0.0004
IOA	0.3948
LMI	0.5749
MBE	-0.0004
NMBE	0.1127

In the present study, a total of 344 datasets have been scrutinized, each of which has exhibited either of the two modes of failure, namely, failure and stable in 176 (51%) and 168 (49%) cases, respectively. It has been observed, through the analysis depicted in Fig. 11(a), that these modes of slope stability have been quite evenly distributed. Moreover, the effectiveness and accuracy of the proposed multi-variable regression methodology have been shown in Fig. 11(b), which presents a comparative analysis between the measured, or actual, FOS data and the obtained outcomes. The multi-variable regression approach has demonstrated good agreement with the measured data, thereby confirming its utility in predicting slope stability. Furthermore, some loss functions are utilized to determine the error of calculated values. The results of these loss functions and statistical indexes are presented in Table 11. As can be seen, the values of these functions are close to zero, which have shown the reliable results with high accuracy and reliability. Thus the empirical formula can be utilized to predict the FOS based on defined geotechnical and geometrics characteristics of soil materials.

3.2 Developing predictive networks using supervised algorithms

The implementation of smart algorithms for prediction is a key aspect of the study. These algorithms have the capability to process large amounts of data and identify complex patterns and relationships among variables that may not be apparent through traditional analysis methods. By harnessing the power of ML and predictive algorithms, the study is able to provide more accurate and reliable predictions of slope stability, which is essential for effective risk management and hazard prevention.

In geotechnical projects characterized by intricate geological conditions and a multitude of essential input factors, supervised learning algorithms such as machine

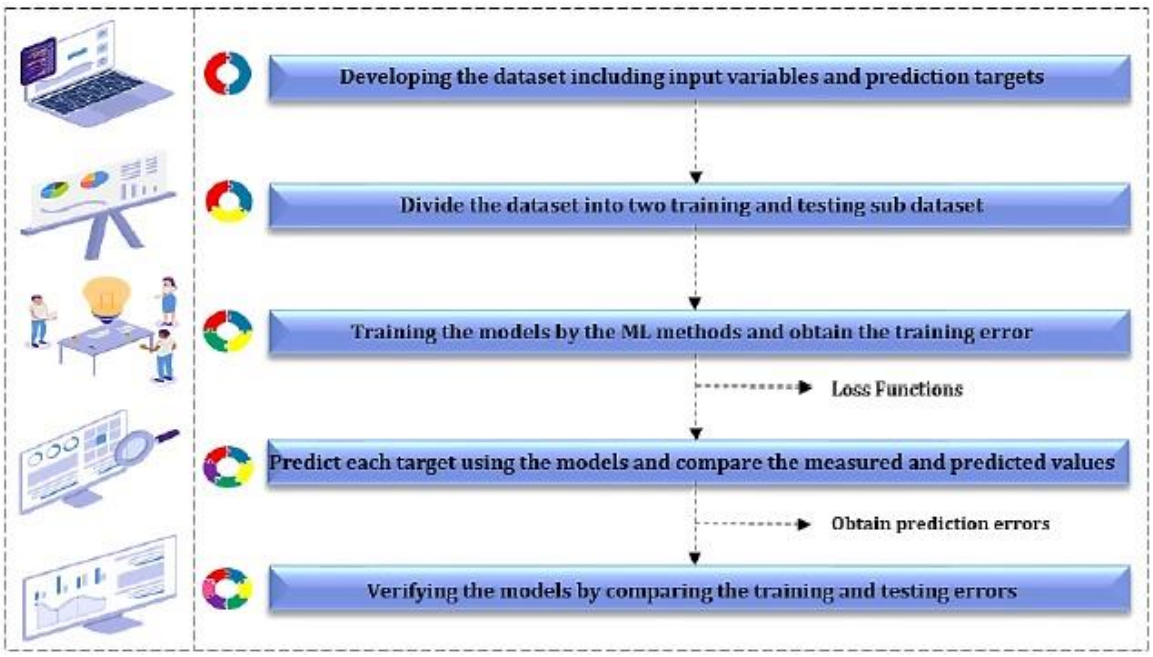

Fig. 12 Overall schematic of application supervised learning algorithms (Samadi *et al.* 2023a)

learning, deep learning, genetic approaches, neural networks, and fuzzy-based models have seen a surge in adoption. The amalgamation of these supervised learning algorithms has demonstrated its effectiveness in elevating the precision and productivity of FOS estimation models tailored for geotechnical applications.

In this section, a concise introduction to several widely used algorithms for FOS estimation, including Ls-SVM, TSFL, FFNN, GEP, and BPNN are presented. These algorithms are trained and tested using a Five-Step Algorithm that is prevalent in all artificial intelligence techniques, as illustrated in Fig. 12.

In assessing the precision and effectiveness of the created models, a range of loss functions and statistical metrics have been proposed. These metrics serve to gauge the disparity between the predicted and true FOS values, as well as to evaluate the forecasting capabilities of the algorithms.

As a limitation of applying ML algorithms in prediction of factor of safety in rock slopes, several items should be mentioned as follow.

Rock slope stability is influenced by a multitude of complex geotechnical processes, such as weathering, fracturing, and seismic activity, which may be challenging to capture and represent accurately in a ML model. ML models require large amounts of high-quality data to train, validate, and test the model. In the case of rock slopes, there may be limited data available, especially when considering factors such as geological variability, weather conditions, and human-induced changes.

3.2.1 FFNN

The FFNN algorithm, for example, is one of the neural networks that has been widely used for FOS estimation in geotechnical projects. It is characterized by moving in a single direction, progressing through hidden layers to estimate output factors. The learning process of FFNN involves adjusting weights and biases of the nodes to optimize the model's output (Andreas 1994).

This algorithm is chosen for analysis because of the following reasons:

- Universal approximation: FFNNs are able to approximate any continuous function to arbitrary precision, making them highly flexible in modeling various types of complex systems.
- Capability for non-linear function approximation: FFNNs can model non-linear relationships between input and output variables, which makes them suitable for a wide range of applications in many fields.
- Support for parallel processing: FFNNs can be implemented in a parallel architecture, which allows for efficient processing of large amounts of data in real-time.
- Robustness to noise: Because FFNNs are trained using data samples, they are able to learn from noisy data by extracting meaningful patterns from the noise.
- Ease of training: This algorithm is a simple and effective algorithm for adjusting the weights and biases of the network.
- Capability for adaptive learning: FFNNs can learn and adapt to new data, making them useful for dynamic systems where the environment changes over time.
- Compatibility with many data types: FFNNs can be used with a wide range of data types, including images, audio, and text, enabling them to be used in diverse applications such as image recognition, voice recognition, and text classification.

3.2.2 BPNN

The BPNN is a type of neural network that comprises an input layer, hidden layer, and output layer. The output layer determines the deviation of the model's predicted results

from the actual data, which is then propagated back to the input layer for weight adjustment (Stuart 1973).

Both the hidden and output layers incorporate bias with a weight of one. This network operates in three phases: sending, backpropagation, and weight updating. During the first phase, the signal is sent from the input layer to the output layer. In the second stage, the error from the output layer is back propagated to the input layer for adjustment of the weights. The third stage comprises the updating of the determined weights. Backpropagation neural networks have become one of the most widely used artificial intelligence techniques due to their fast processing, high flexibility, and lack of requirements for special attention to features during the training stage (Paul 1982).

This algorithm is chosen for analysis because of the following reasons:

- The backpropagation neural network has been renowned for its capacity to provide accurate predictions for various applications.
- It is a type of supervised learning algorithm whereby the training data must have known labels, thus enabling the network to update internal parameters by minimizing the prediction error.
- The output of the network is determined by the weighted sum of the inputs coupled with activation functions in the hidden layers that improve the flexibility and accuracy of the model.
- Backpropagation neural networks have been widely utilized in various fields, including geotechnics, tunnelling, and rock mechanics, due to their ability to learn from experience and generalize from previously seen epochs.

3.2.3 Ls-SVM

Ls-SVM is frequently utilized for prediction and statistical modeling. Ls-SVM is often used for prediction target factor because it offers several advantages over traditional support vector machine (SVM). This method is a variant of SVM, which represent a collection of closely related supervised learning techniques that analyze data and identify patterns for classification and regression analysis. The Ls-SVM classifier is a class of kernel-based learning methods that was first introduced by Suykens and Vandewalle (1999). Three types of kernel-based functions are commonly used in these methods, which include linear, polynomial, and Gaussian kernels. Kernel-based functions differ in terms of hyperplane decision boundaries that are established between the data classes. Results have indicated that the Gaussian kernel outperforms the linear and polynomial kernels in terms of accuracy, albeit at the expense of relatively high computational costs (Guo *et al.* 2011). Therefore, the current study employs a Gaussian kernel-based Ls-SVM to evaluate the model predictions.

This algorithm is chosen for analysis because of the following reasons:

- LS-SVM is a linear regression method that finds the hyperplane that best separates the data points. It has a closed-form solution that is more efficient than traditional SVMs, which require iterative solutions.
- LS-SVM mitigates the likelihood of data overfitting by incorporating a regularization parameter that governs the model's complexity, thus safeguarding against noise overfitting.
- LS-SVM is well-suited for managing extensive datasets due to its utilization of a kernel trick, enabling data transformation into a higher-dimensional space. This feature enhances its adaptability in dealing with datasets that are non-linearly separable.
- LS-SVM is underpinned by a robust theoretical framework that ensures its convergence and optimality, subject to specific conditions.

3.2.4 TSFL

Takagi and Sugeno (1985) introduced the TSFL model as a systematic method for constructing fuzzy rules based on a given input-output dataset. A standard TS fuzzy rule is structured as follows:

If X is A and Y is B, then Z equals $f(X,Y)$

Here, A and B represent fuzzy sets, and $Z = f(X,Y)$ denotes a specific function. Typically, $f(X,Y)$ is a polynomial that includes the input variables X and Y. However, any function that accurately represents the desired output within the fuzzy region outlined by the rule's condition can be used as $F(X,Y)$. This model is chosen for its application of linear weighted mathematical expressions and its flexibility in adapting to individual input methodologies within Sugeno fuzzy systems. The output in this research is a weighted average, defined as

$$Z = \frac{\sum W_i f_i\,(X,\ Y)}{\sum W_i} \tag{2}$$

Where W_i represents the firing strength of the i^{th} output. The procedure that is applied to transform crisp input values into linguistic variables is referred to as Fuzzification, and this method precisely expresses the crisp inputs in linguistic terms.

This algorithm is chosen for analysis because of the following reasons:

- Widely utilized: This particular type of fuzzy inference system is extensively used and has been the subject of extensive study and research.
- Enhanced versatility: It possesses the ability to handle a wide range of applications, particularly geotechnical projects, effectively managing complex and non-linear issues.
- Superior accuracy: The fuzzy logic system of this kind delivers more precise results by effectively handling intricate systems. This quality proves particularly beneficial in control systems, decision-making processes, and pattern recognition applications.
- Easy implementation: Implementation of this system is relatively simple and does not necessitate a large amount of data to develop accurate models.
- Solid theoretical underpinning: The foundation of these fuzzy logic systems is robust and thoroughly comprehended, making them highly reliable and credible for real-world use.

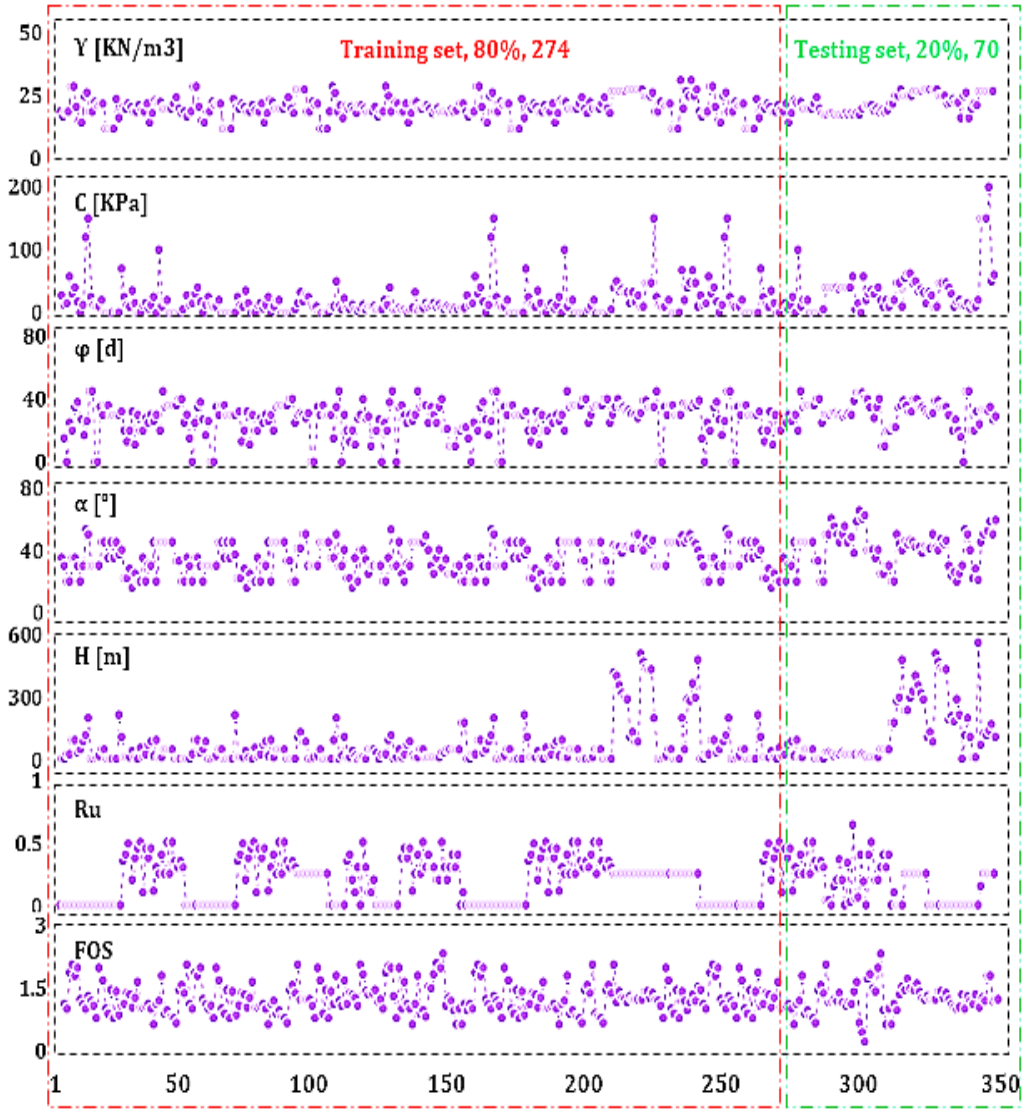

Fig. 13 the order of input and output variables to train and test the supervised networks

3.2.5 GEP

Ferreira (2001) has introduced a genetic algorithm called GEP that is based on genetic programming (GP) and genetic algorithm (GA). Gene expression programming is a genotype-phenotype multi-genic system that combines the strengths of genetic programming and the simplicity of the genetic algorithm. Unlike its predecessors, GEP encodes multiple evolutionary algorithms as linear structures known as chromosomes that are composed of genes with equal length. The determinants of GEP are the chromosomes and the expression tree (Ets). The algorithm employs two languages, the language of genes and the language of expression trees. The sequence of genes can be deduced from the expression tree, and vice versa, using the Karva language. GEP has two domains, the head and the tail, where the head encodes the chosen functions and variables to solve problems, while the tail provides a terminal reservoir to ensure that all programs produced by GEP are error-free (Ferreira 2001).

This algorithm is chosen for analysis because of the following reasons:

- GEP provides an innovative solution to complex problems due to its unique approach to encoding and decoding information. By encoding evolutionary algorithms as linear structures called chromosomes, genes with equal length can be composed to form multigenic systems. This allows for the complexity of genetic programming combined with the simplicity of the genetic algorithm.
- The expression tree, one of the two determining factors of GEP, is crucial to understanding how GEP works. The expression tree employs two languages, the Karva language and the language of genes, whereby the sequence of genes can be derived from the expression tree, and vice versa.
- The head and tail are two domains of GEP that serve distinct purposes. The head is responsible for encoding the specific functions and variables used in problem-solving, while the tail provides a terminal reservoir to ensure that all programs produced by GEP are free of errors.

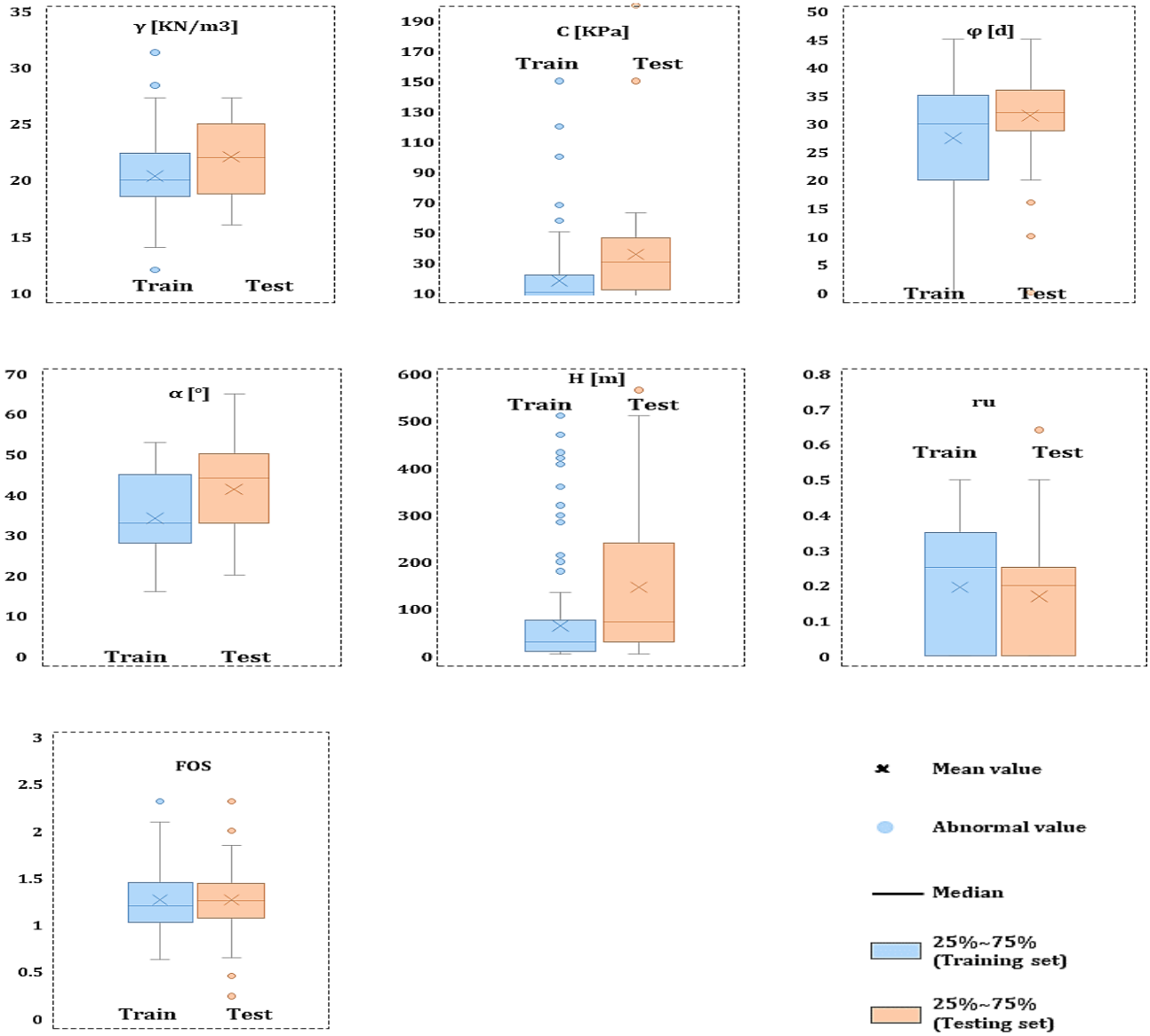

Fig. 14 Boxplots of input(s) and output factors for training and testing sub-sets to develop and train supervised learning algorithms

- Overall, the notation of GEP is considered bilingual, offering a unique and effective strategy for tackling complex problems.

3.3 Results of ML al-based algorithms

In this research, prediction networks were devised to anticipate the factor of safety in slope stability analysis. To achieve this, four distinct methods including ML, fuzzy-based, and genetic algorithms were utilized and trained utilizing a blend of geotechnical and geometric parameters as inputs, with FOS values as outputs. It's crucial to highlight that the accuracy of AI-generated results heavily relies on the quality and arrangement of the training data. Hence, randomizing the data order was implemented before network training, and certain neural network parameters were normalized (refer to Fig. 13). To gauge the reliability of the forecast models employed for slope stability evaluation, an extensive database consisting of 344 slope cases analyzed for circular failure mechanisms was utilized. This dataset was divided into two subsets, with 80% (274 data points) used for training and the remaining 20% (70 data points) designated for testing the supervised ML models.

Fig. 14 illustrates boxplots for each parameter within the training and testing subsets. These boxplots depict the upper and lower boundaries of the 25th and 75th percentiles for each correlation, along with the interquartile range representing the spread between the upper and lower limits of the box. The median of the sample is indicated by a central line within each box. Data pertaining to ϒ and C are observed to have a median that is relatively centered within the box, while data for other parameters exhibit a skewed distribution. The whiskers, extending from the boxes above and below, are determined by the farthest data within the whisker range and span from the endpoints of the

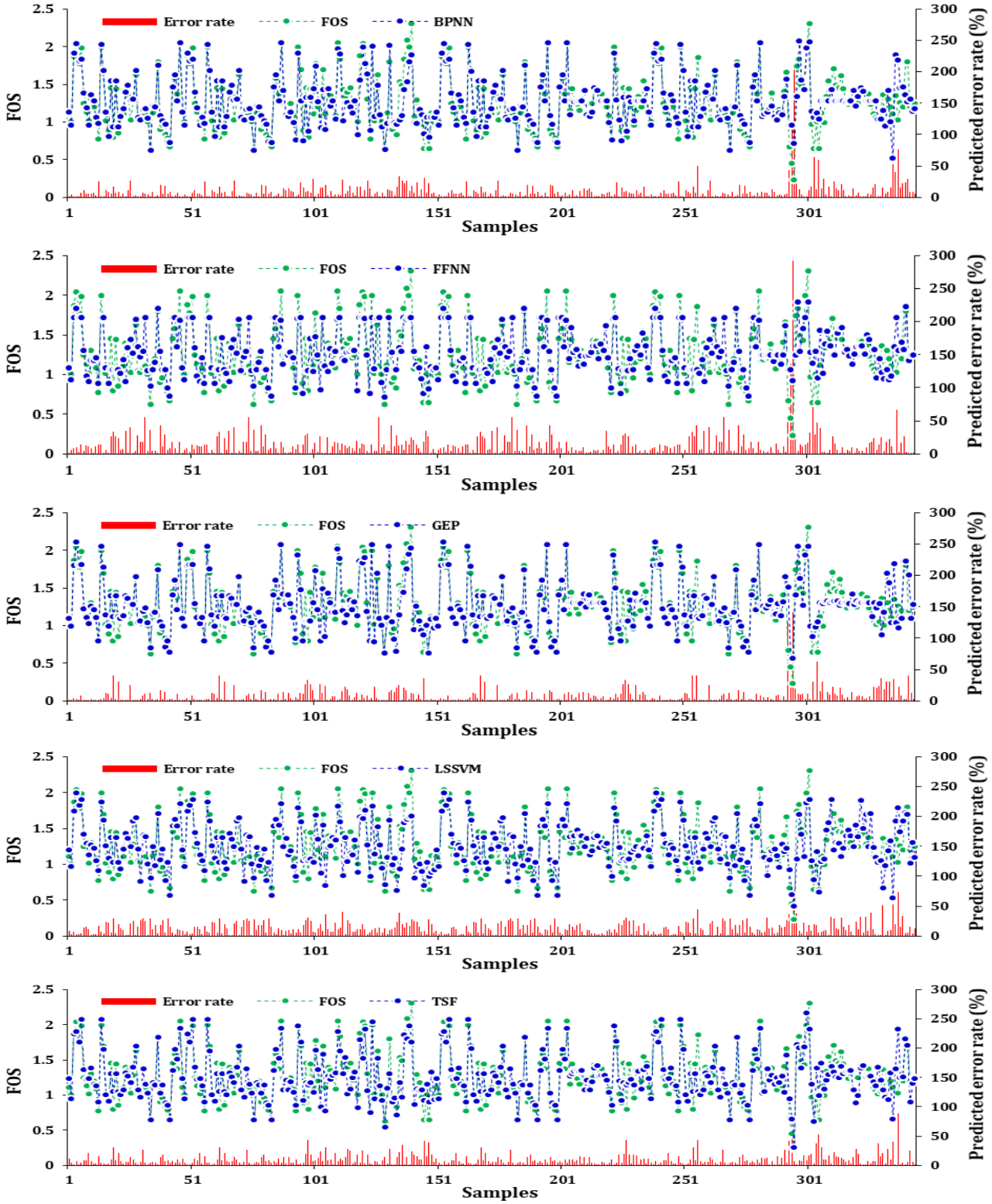

Fig. 15 Comparison between predicted values of FOS using five types of supervised learning algorithm and measured one

interquartile range.

The optimization process involved identifying the optimal values or states of the hyperparameters for each ML model, accomplished through a trial-and-error approach aimed at fine-tuning the hyperparameters.

The obtained results demonstrate that the predicted FOS parameters yielded by the network showed strong correspondence with the measured data. Fig. 15 shows a comparison between the measured and predicted values of FOS, which indicates the network's ability to accurately predict sudden changes in target values. In addition, the relationship between the actual and predicted values of FOS

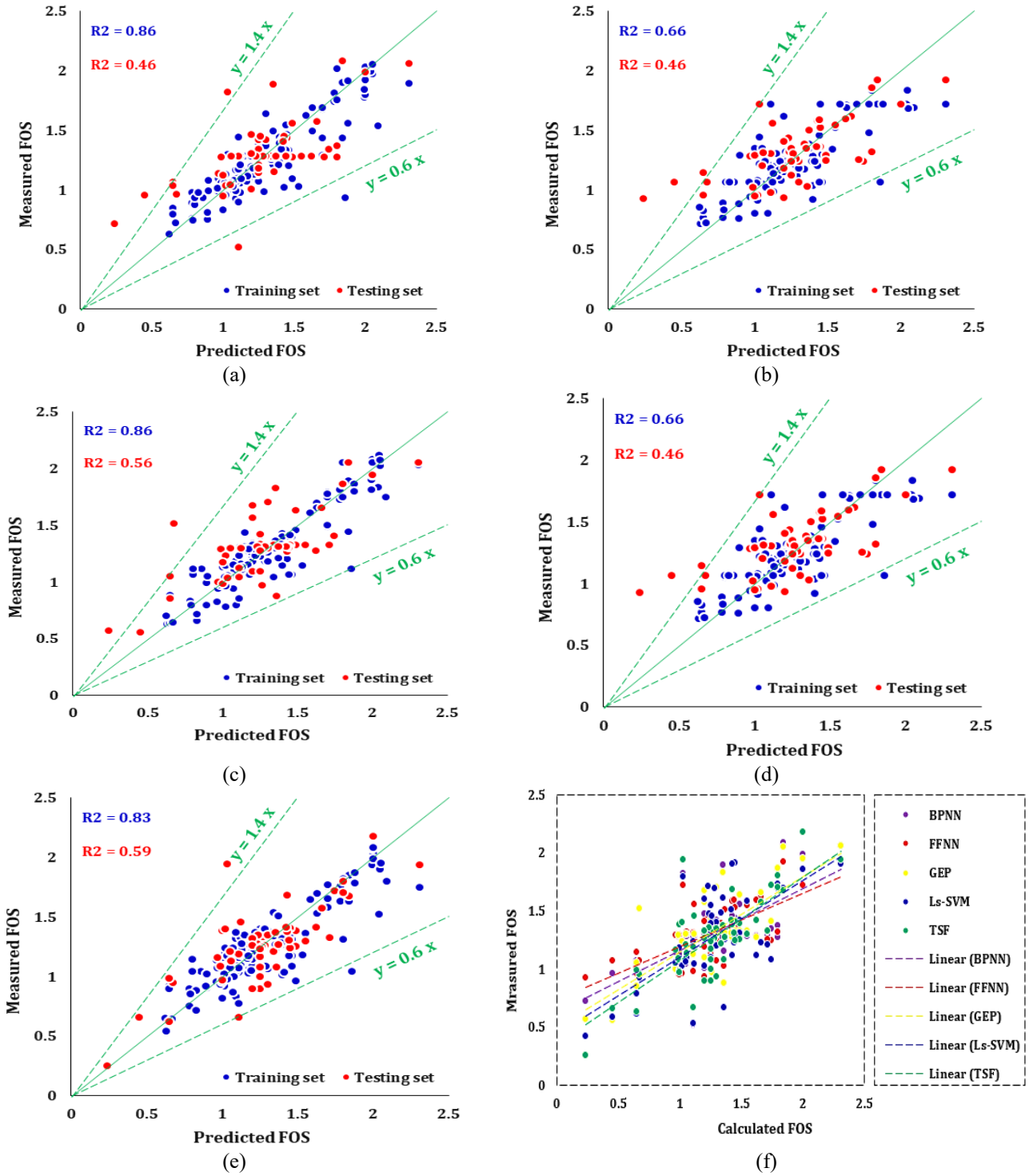

Fig. 16 The correlation between the measured and predicted results of FOS based on supervised learning algorithms, (a) BPNN, (b) FFNN, (c) GEP, (d) Ls-SVM, (e) TSF and (f) testing subset of all models

is presented in Fig. 16.

In the current research, loss functions were implemented as a tool for evaluating the ML networks' accuracy. Loss functions enable one to compute the degree of deviation of the predicted outcomes obtained during the ML process from the actual measured values. The adoption of loss functions in this study promotes a quantitative approach towards the assessment of the predictive capacity of the ML models.

Table 12 furnish the findings of the loss functions assessment for the training and testing subsets' FOS parameter. The outcomes indicated that the computed values of the various loss functions were consistent, illustrating excellent results in predicting the values of FOS based on the input data derived from the physical and geotechnical features. This foundation of evaluation is a crucial step towards determining the potential for application of ML techniques in the field of geotechnical engineering.

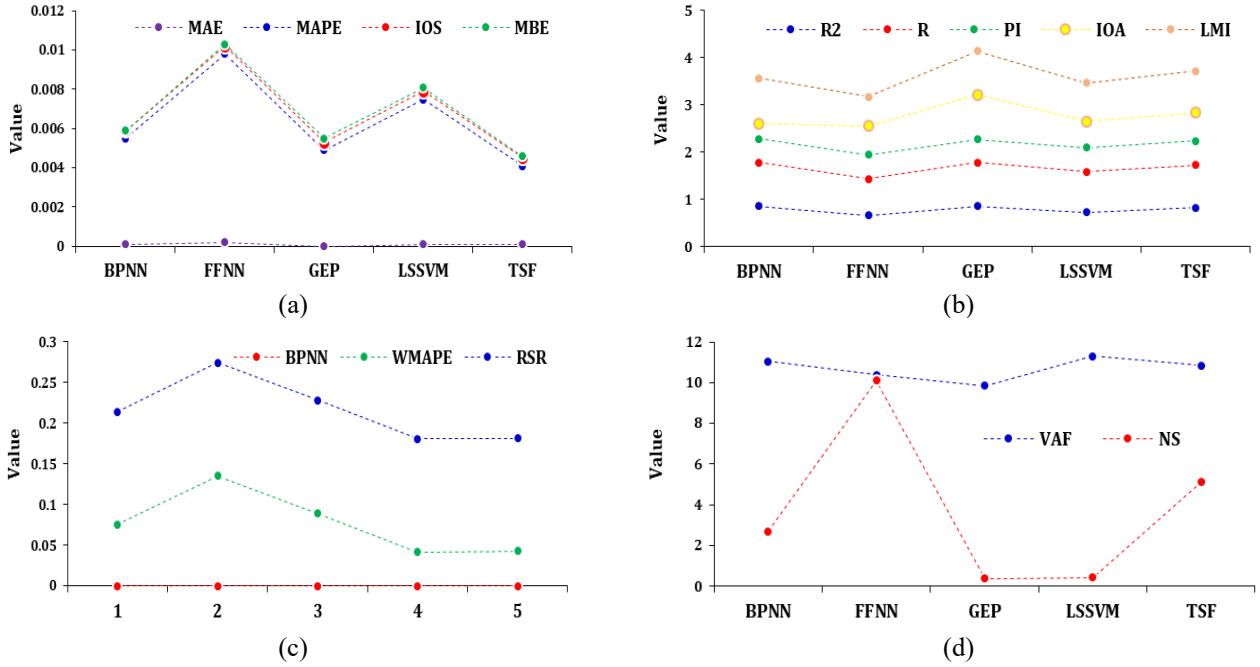

Fig. 17 Results and comparison of loss functions in the development of supervised learning methods for FOS

To expand on the research findings, Fig. 17 present a visual comparison between different types of loss functions for predicting the values of FOS. The graphs plotted reveal the results of the loss functions evaluation on the predictive performance of the models. The comparative analysis highlights the superior prediction ability of the ML networks, which showcases its potential to revolutionize the field of geotechnical engineering.

Overall, the adoption of loss functions and the subsequent evaluation of the ML models' accuracy displayed in this study demonstrate the potential of these techniques to accurately predict the parameters for future slope stability analysis. The techniques employed in this study could set the precedent for further research in the integration of ML models in geotechnical applications.

4. Sensitivity analysis

It is worth to mention that additionally to correlation matrix, the authors applied sensitivity analysis which is an acceptable option to determine the effect of each factor on target parameter. This decision is supported by the finding that slope height is a particularly influential parameter in slope stability analysis as demonstrated by the results of multi-factor sensitivity analysis, as depicted in Fig. 18. This aligns closely with the significance attributed to slope height in our study.

Thus the multi-factor sensitivity analysis provides a comprehensive understanding of the impact of each factor on slope stability. This in-depth analysis allows researchers and engineers to identify the most influential factors and prioritize them in their assessments and risk management strategies. By gaining a better understanding of the complex interactions among various parameters, practitioners can make more informed decisions and implement more effective slope stability measures.

In this study, we utilized the mutual information (MI) technique to conduct sensitivity analysis. MI is a feature selection method based on information theory, which uses information gain to build decision trees. It quantifies the extent to which one variable can be inferred from observations of another. MI is straightforward to use with categorical input and output data, and can also be adapted for numerical data, despite its original design for textual data. The effectiveness of MI can be evaluated by the reduction in entropy. As shown in Eq. (3), the MI score is a positive integer between zero and infinity. A high MI value signifies the feature's importance in model training, while a low MI score, such as 0, indicates limited or no correlation between the attribute and the objective.

The MI scores for all inputs are presented in Fig. 18, which indicates the significant impact of the φ and H parameters on the FOS, while also highlighting the influence of other parameters on the FOS properties.

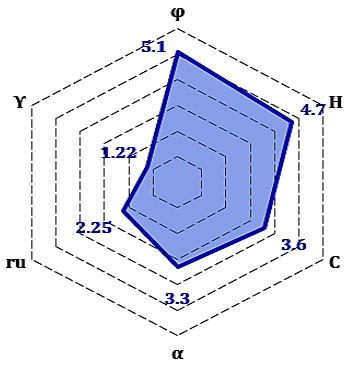

Fig. 18 Multi-factor sensitivity score of input parameters

Table 12 The results of loss functions in the development of supervised learning methods for FOS

	BPNN	FFNN	GEP	LSSVM	TSF
RMSE	0.001	0.001	0.0006	0.004	0.006
MAE	0.0001	0.0002	0.0000	0.0001	0.0001
R^2	0.86	0.66	0.86	0.73	0.83
R	0.92	0.78	0.92	0.86	0.90
MAPE	0.0054	0.0096	0.0049	0.0074	0.0040
WMAPE	0.0753	0.1351	0.0893	0.0416	0.0426
VAF	11.0339	10.3771	9.8451	11.2967	10.8385
PI	0.5099	0.5033	0.4980	0.5125	0.5079
RSR	0.1390	0.1390	0.1390	0.1390	0.1390
NS	-2.7047	-10.1074	-0.3928	0.4311	-5.1123
BF	0.0030	0.0029	0.0029	0.0029	0.0028
IOS	0.0004	0.0004	0.0004	0.0004	0.0004
IOA	0.3216	0.6157	0.9404	0.5474	0.5990
LMI	0.9558	0.6201	0.9264	0.8171	0.8890
MBE	0.0000	0.0001	0.0002	-0.0002	-0.0001
NMBE	0.0123	0.0039	0.0148	0.0561	0.0004

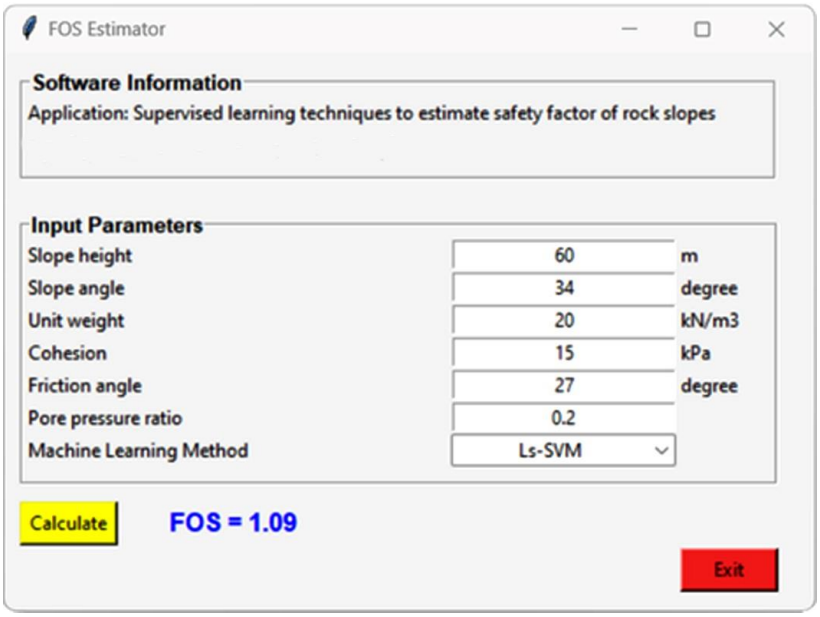

Fig. 19 GUI of the ML–based models for estimating the FOS of slopes

$$MI\ (feature; target) = Entropy\ (feature) - Entropy\ (feature \mid target) \quad (3)$$

5. Graphical user interface

The use of statistical measures and loss functions to determine the accuracy of ML algorithms further enhances the reliability and credibility of the study. The close-to-zero results of the loss functions indicate the high accuracy of the models, validating the efficacy of the ML algorithms in predicting slope stability. This rigorous evaluation process demonstrates the robustness of the approach and instills confidence in the accuracy of the predictive models developed in the study.

Additionally, the development of an easy-to-use GUI (graphical user interface) software is a significant contribution to the field. The user-friendly interface allows engineers and researchers to easily input data, run analyses, and visualize results without the need for extensive programming or technical expertise. This accessibility makes the findings of the study more applicable and useful to a broader audience, facilitating the adoption of the new approach in real-world slope stability assessments and engineering projects.

As an easy-to-use method for estimating slope FOS, graphical user interfaces (GUIs) may provide models based on ML. All six ML algorithms explored in this research are included in the program. There's no necessity to retrain the prediction models for assessing the FOS of slopes since they've already been trained on experimental data points.

The user interface has been meticulously designed for ease of use (as depicted in Fig. 19). Once the user inputs parameters into the GUI, the trained ML algorithms can swiftly estimate the output parameter (FOS). In comparison to prior methods, the GUI enables highly accurate estimation of slope FOS in a remarkably brief timeframe and at minimal expense. Moreover, it holds promise as a learning platform for those interested in collecting slope FOS data. Each ML model's processing time varied, ranging from 8 seconds to 184 seconds.

6. Conclusions

This current research proposes six different supervised and unsupervised learning models that aim to predict slope stability by using 344 datasets that have been assessed using PLAXIS software. The six input factors that the study takes into account are c, α, ϒ, h, φ, and r_u, while the target variable is the FOS.

When compared to previous approaches, the FOS of slopes may be estimated with high accuracy using the GUI in a very short amount of time and at a cheap cost.

It is suggested that future research utilizing the models presented in this study explores the most accurate algorithm and the most effective parameters for slope stability prediction. Besides, to address the various challenges faced in this domain, the models' predictive ability in geotechnical and geological issues must be examined and discovered.

In conclusion, the unique contribution of this study lies in its alternative approach to slope stability analysis with enhanced accuracy and applicability. By combining a new empirical equation, smart algorithms for prediction, easy-to-use GUI software, and rigorous evaluation of ML algorithms, the study offers a comprehensive and sophisticated methodology for assessing and predicting slope stability. This approach has the potential to revolutionize current practices in slope stability analysis and engineering, ultimately leading to more effective and reliable solutions for managing slope-related hazards.

The database utilized in this study carries several limitations. Specifically, our investigation aims to ascertain the factor of safety for rock slopes by leveraging both the geotechnical properties of materials along the slope and the geometric properties of the slopes themselves. To bolster the comprehensiveness and applicability of the ML-based and supervised models introduced in this study, expanding the database is imperative. The authors are actively engaged in enhancing the database by integrating data from various rock slope cases. It is expected that developing ML and Deep Learning models based on this expanded dataset will yield significantly more efficacious results. Furthermore, it's worth mentioning that the proposed models might find utility in similar slopes and the geotechnical parameters of materials along these slopes. It is suggested that forthcoming research concentrate on further enriching the database by assimilating data from additional slopes, while also encompassing a wider array of geotechnical conditions and geometric properties. Moreover, future investigations could delve into employing alternative ML algorithms to augment the predictive capabilities of the study.

Data availability

The datasets generated and/or analyzed during the current study are available in the following address: https://mega.nz/file/PXhggKrZ#p6HIkmctZVRw7y_ofCSS6-4WFvRvf4o_9NDg3lVwn1I.

Acknowledgements

This work was supported by General Programs of the National Natural Science Foundation of China (Grant nos. 51774184), Excellent Research Team Fund in North China University of Technology (Grant no. 107051360019XN134/017), and Scientific Research Fund in North China University of Technology (Grant no. 110051360002).

This study is supported via funding from Prince Satam bin Abdulaziz University project number (PSAU/2024/R/1445).

References

Andreas. Z. (1994), "Simulation neuronaler netze-simulation of neural networks", Addison-Wesley, **1**(5.3),

Ahangari, N., Pusatli, T., Chengyong, J., Chen, J., Cemiloglu, A., Azarafza, M. and Derakhshani, R. (2022), "Application of ML techniques for the estimation of the safety factor in slope stability analysis", *Water*, **18**(22), 3743. https://doi.org/10.3390/w14223743.

Bai, G., Hou, Y., Wan, B., An, N., Yan, Y., Tang, Z., Yan, M., Zhang, Y. and Sun, D. (2022), "Performance evaluation and engineering verification of ML based prediction models for slope stability", *Appl. Sci*., **12**(15), 7890. https://doi.org/10.3390/app12157890.

Bishop, A.W. and Morgenstern, N. (1960), "Stability coefficients for earth slopes", *Geotechnique*, **10**(4), 129-153. https://doi.org/10.1680/geot.1960.10.4.129.

Chakraborty, A. and Goswami, D. (2017), "Prediction of slope stability using multiple linear regression (MLR) and artificial neural network (ANN)", *Arab. J. Geosci*., **385**. https://doi.org/10.1007/s12517-017-3167-x.

Das, S.K., Biswal, R.K., Sivakugan, N. and Das, B. (2011). "Classification of slopes and prediction of factor of safety using differential evolution neural networks", *Environ. Earth. Sci*., **64**(1), 201-210. https://doi.org/10.1007/S12665-010-0839-1.

Eberhardt, E. (2003), "Rock slope stability analysis–utilization of advanced numerical techniques", Earth and Ocean sci. at UBC., **41**.

Ferreira, C. (2001), "Gene expression programming: A new adaptive algorithm for solving problems", *Comp. Sys*., **13**(2), 87-129. https://doi.org/10.48550/arXiv.cs/0102027.

Guo, J.R., He, Y.G. and Liu, C.Q. (2011), "Nonlinear correction of photoelectric displacement sensor based on least square support vector machine", *J. Cent. South. Univ*., **18**(5), 1614-1618. https://doi.org/10.1007/s11771-011-0880-6.

Hoang, N.D. and Pham, A.D. (2016). "Hybrid artificial intelligence approach based on metaheuristic and ML for slope stability assessment: A multinational data analysis", *Exp. Syst. Appl*., **46**, 60-68. https://doi.org/10.1016/j.eswa.2015.10.020

Jagan, J., Meghana, G. and Samui, P. (2016), "Determination of stability number of layered slope using ANFIS, GPR, RVM and ELM", *Int. J. Comput. Res*., **23**(4), 371-393.

Karir, D., Ray, A., Bharati, A.K., Chaturvedi, U., Rai, R. and

Khandelwal, M. (2022), "Stability prediction of a natural and man-made slope using various ML algorithms", *Transport. Geotech*., **34**, 100745. https://doi.org/10.1016/j.trgeo.2022.100745.

Li, S., Zhao, H.B. and Ru, Z. (2013), "Slope reliability analysis by updated support vector machine and Monte Carlo simulation", *Nat. Hazards*, **65**, 707-722. https://doi.org/10.1007/s11069-012-0396-x.

Liu, Z., Shao, J., Xu, W., Chen, H. and Zhang, Y. (2014), "An extreme learning machine approach for slope stability evaluation and prediction", *Nat. Hazards*, **73**(2), 787-804. https://doi.org/10.1007/s11069-014-1106-7.

Liu, Y.C. and Chen, C.S. (2007), "A new approach for application of rock mass classification on rock slope stability assessment", *Eng. Geol*., **89**(1-2), 129-143. https://doi.org/10.1016/j.enggeo.2006.09.017.

Lu, P. and Rosenbaum, M.S. (2003), "Artificial neural networks and grey systems for the prediction of slope stability", *Nat. Hazards*, **30**(3), 383-398. https://doi.org/10.1023/B:NHAZ.0000007168.00673.27

Mahmoodzadeh, A., Mohammadi, M., Hama Ali, H., Ibrahim, H., Abdulhamid, S. and Nejati, H. (2021), "Prediction of safety factors for slope stability: comparison of ML techniques", *Nat. Hazards*, **111**, 1771-1799. https://doi.org/10.1007/s11069-021-05115-8.

Omar, M., Che Mamat, R., Abdul Rasam, A.R., Ramli, A. and Samad, A. (2021), "Artificial intelligence application for predicting slope stability on soft ground: A comparative study", *Int. J. Adv. Technol. Eng. Explor*., **8**(75), 362-370. https://doi.org/10.19101/IJATEE.2020.762139.

Pantelidis, L. (2009), "Rock slope stability assessment through rock mass classification systems", *Int. J. Rock Mech. Min. Sci*., **46**(2), 315-325. https://doi.org/10.1016/j.ijrmms.2008.06.003.

Samadi, H., Hassanpour, J. and Farrokh, E. (2021), "Maximum surface settlement prediction in EPB TBM tunneling using soft computing techniques", *J. Phys.: Conference Series*, **1973**(1), 012195. http://doi.org/10.1088/1742-6596/1973/1/012195.

IC